Asymmetric butterfly velocities in local time-independent Hamiltonians

The butterfly velocity v_B is the velocity at which initially local operators spread. In many 1-D systems this velocity is independent of the direction of spreading. This need not be the case. In fact, with arbitrarily nonlocal Hamiltonians, or arbitrarily deep circuit models, the ratio of the two butterfly velocities may be made arbitrarily large. We provide a class of circuits whose limiting behavior shows this arbitrarily large ratio. We also describe a local Hamiltonian with an asymmetric v_B, presenting various methods to measure the asymmetry.

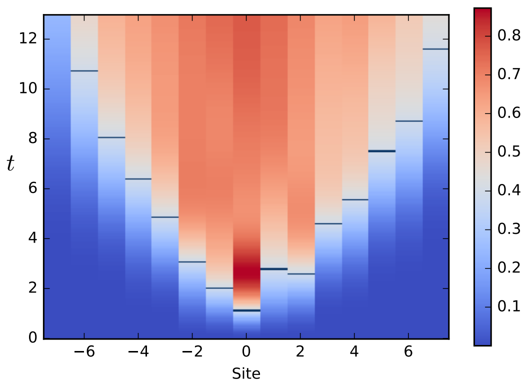

FIG. 1. Illustration of the initially local operator. The bars indicate the time at which the OTOC passes 0.4, to emphasize the asymmetry.

I. INTRODUCTION

If we label $1 \ldots L$, then even and odd sites switch. Be careful!

Thermalization is important because...

Asymmetric transport is seen in “staircase” and “glider” circuits, but we wanted to show it is also possible in time-independent Hamiltonians.

In a 1-D circuit, how asymmetric can the spreading be?

On the edge of a 2-D system, spreading can be chiral even with a finite circuit depth [?].

To be completely chiral with only 1 dimension, the circuit will have to be of infinite depth.

Given a constraint on the depth, how asymmetric can the spreading be?

In this paper we will start by discussing a local Hamiltonian with asymmetric spreading. We show that it is a general Hamiltonian, and provide multiple methods for measuring v_B for left and right spreading. We then discuss staircase circuits in the small- and large-staircase limit and show that in the latter limit the circuit is completely chiral.

Throughout this paper we will use different methods to measure v_B. For the Hamiltonian system, we use two methods, both directly related to the spreading of operators. The first is non-local, measuring the velocity of the peak in the right- and left-weights. The other defines velocity-dependent Lyapunov exponents from the early-time OTOCs. For the circuit we extract v_B from the growth rate of the entanglement entropy.

CONTENTS

II. LOCAL HAMILTONIANS

In order to define a local Hamiltonian with asymmetric spreading, we have to move away from 2-site interactions because these will have to be symmetric. The space of 3-site Hamiltonians is large ($q^6 = 64$) so we restrict to SU(2)-symmetric terms.

This space is still large Does it matter how large?, but we know we want Hamiltonians that are different in opposite directions. If we restrict further to Hamiltonians antisymmetric under inversion of the spin chain, we are left with only one option, the triple product of spins. The Hamiltonian on the full chain is then

$$H = \sum_{i=1}^{L-2} \mathbf{S}_i \cdot (\mathbf{S}_{i+1} \times \mathbf{S}_{i+2})$$

Since this connects 2-nearest neighbors, even and odd sites will behave differently at early time. For example, first order perturbation theory will connect site 1 to sites 2 and 3, while second order perturbations connect site 1 to sites 4 and 5. This effect will come up when looking at spreading of operators.

A. Degeneracy and Generality

As is, the model is not general, presenting a large degeneracy at $E = 0$. This is an effect of various antisymmetries in the model, which we will call R_i. Each of these operators maps between states of opposite energy. Ref. [**?**] shows that each Tr R_i provides a lower bound on the $E = 0$ degeneracy, which we will call N_0. Writing the $E = 0$ states as $|\alpha\rangle$,

$$\text{Tr } R_i = \sum_{\alpha=1}^{N_0} \langle\alpha|R|\alpha\rangle, \tag{1}$$

But from $R_i^2 = 1$ we have

$$\langle\alpha|R_i|\alpha\rangle = \pm 1. \tag{2}$$

Thus Tr $R_i < N_0$.

From the design of the model, one such R_i is the inversion operator, I. This can be composed with parity operators such as $P_X = \prod_i X_i$ that commute with both H and I to form new R_i. Neither operator accounts for the entire degeneracy, but $\text{Tr}\, I = N_0$ for odd L. If we break the SU(2) symmetry to U(1) but leave the inversion symmetry intact then $\text{Tr}\, I$ is exact. If we add a uniform field in the Z direction, then IP_X is an antisymmetry but I is not. In this case $\text{Tr}(IP_X)$ is exact. Taken together, these facts imply that the extra degeneracies for odd L come from mixing of the SU(2) symmetry and inversion antisymmetry.

We can fully break this degeneracy within each U(1) block by introducing a random field in the Z direction, so the total Hamiltonians is

$$H = \sum_{i=1}^{L-2} \mathbf{S}_i \cdot (\mathbf{S}_{i+1} \times \mathbf{S}_{i+2}) + \sum_{i=1}^{L} h_i S_i^z, \tag{3}$$

where each h_i has a uniform probability distribution on $[-h, h]$. This field breaks the SU(2) symmetry but leaves the U(1) subgroup intact.

For sufficiently large h the model becomes localized. In the large-L limit the transition from ergodic to localized is a phase transition, described in [**?**]. The transition for the present model can be seen in Fig. 2, showing the ratio of adjacent energy gaps. Note that at smaller L the model also drifts away from GUE statistics at very small h, when the field is no longer large enough to fully lift the $E = 0$ degeneracy.

B. Right-weight peaks

We will measure the asymmetry using two metrics. The first is the weight of all operators with right (left) endpoint on site i, which we will call the right (left) weight. The other is the OTOC. should we define these in this section? Make sure to point out use of initial operators as being on site 0 or $L-1$.

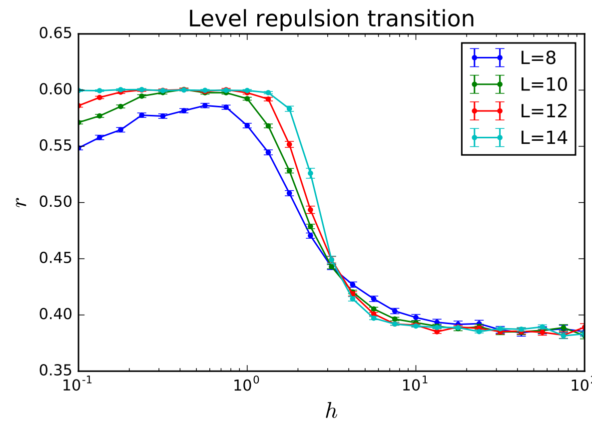

FIG. 2. Phase transition for the model, with level repulsion parameter plotted against field strength. Note that in the thermalizing phase the ratio is 0.6 instead of 0.53 because the statistics are GUE instead of GOE. I think I remember Vedika saying this but I can't find where.

We use the definition of the right weight from [**?**]. An arbitrary operator $\mathcal{O}$ can be decomposed into Pauli strings $\mathcal{O} = \sum_\nu c_\nu \sigma^\nu$ where each string contains one of $\{I, X, Y, Z\}$ acting on each site. As the operator evolves in time, so do the c_ν. The right weight is then

$$\rho_r(i, t) = \sum_\nu |c_\nu(t)|^2 \, \delta(\text{RHS}(\nu) = i), \tag{4}$$

where the delta function ensures that we only count Pauli strings that have their right-most non-identity operator on site i. The left weight $\rho_l(i, t)$ is defined analogously. If $\mathcal{O}$ is initially local on site j then $\rho_r(i, 0) = \rho_l(i, 0) = \delta_{ij}$. As the operator spreads, the support of ρ_r moves right at $v_{B,r}$ and ρ_L moves left at $v_{B,l}$. Operator broadening manifests itself in the support of both weights increasing in size. At late times both weights should vanish near j.

In the thermalizing phase, the right weights peak as the information front passes. Because of the three-site nature of each term in the Hamiltonian, the right weight and OTOC exhibit an "odd-even" effect. It is possible to account for these by averaging judiciously, or by only looking at even (or odd) sites. At $L = 13$, there are enough even sites that the asymmetry can be seen. For a picture of the rights weights with their successive peaks, see Fig. 3.

Fig. 4 shows the peaks traveling ballistically. The peaks reach equivalent sites at later times for the left-moving wave, implying $v_{B,l} < v_{B,r}$. We can extract $v_{B,l}$ and $v_{B,r}$ from these curves by fitting linear functions to the peak timings.

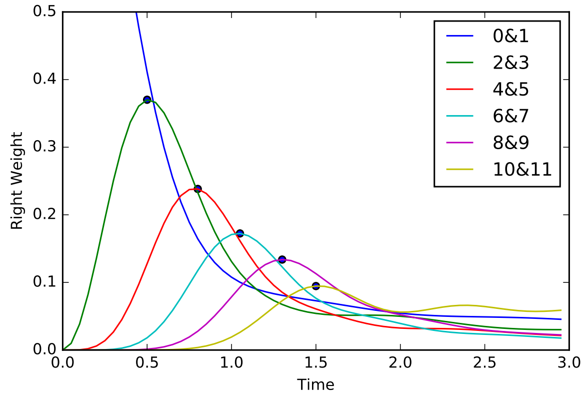

FIG. 3. Right weight at even sites for $L = 13$. The peak travels ballistically. Later peaks are smaller Is this due to broadening?

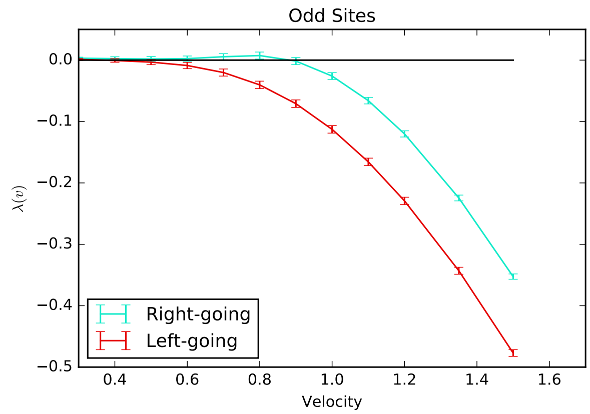

FIG. 5. Velocity-dependent Lyapunov exponents extracted from the OTOC on odd sites. Since $\lambda_r(v) > \lambda_l(v)$, we know $v_{B,r} > v_{B,l}$.

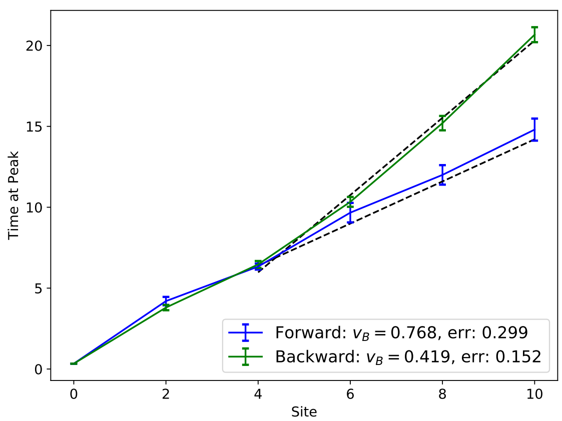

FIG. 4. Time of peak vs. site. Since this is plot of time as a function of distance, the larger slope in the left weight means that v_B is larger for propagation to the right.

C. Velocity-dependent Lyapunov exponents

It is also possible to extract butterfly velocities from the the velocity-dependent Lyapunov exponents, which in turn rely on the OTOC. We define the OTOC as

$$\begin{aligned} C(i,t) &= \frac{1}{2}\langle |[Z_j(t), Z_i(0)]|^2\rangle_{\beta=0} \\ &= 1 - \frac{1}{2^L}\text{Re Tr}\,[Z_j(t)Z_i(0)Z_j(t)Z_i(0)] \end{aligned} \tag{5}$$

where j is the site of the initial operator and the expectation value in the top row is with respect to a thermal ensemble at infinite temperature. We set $j = 1$ to measure $v_{B,r}$ and $j = L$ to measure $v_{B,l}$. The OTOC should be order-1 inside the lightcone and exponentially small outside the lightcone defined by v_B.

From conservation of S_z^{tot}, the Hamiltonian and all relevant operators are block-diagonal, with the size of the i^{th} block being $\binom{L}{i}$. For smaller blocks we can compute the trace directly, but for larger blocks this becomes computationally difficult. We then rely on quantum typicality to approximate the trace in the large blocks. For each disorder realization we replace the trace with an average over expectation values in pure states [**?**]. The pure states are chosen Haar-randomly, and we find that using 5 vectors gives relative errors around 0.05 for all but the smallest blocks.

The VDLEs quantify how fast signals decay along constant-velocity trajectories outside the lightcone. In particular, if the OTOC is measured along the ray defined by each site i at time $t_i = i/v$ for some v, then it should decay exponentially,

$$C(i,t) \sim e^{\lambda(v)t} \quad \text{for} \quad i = vt. \tag{6}$$

Ref. [**?**] gives a thorough explanation of VDLEs. The name comes from the fact that the Lyapunov exponent defines how fast a signal grows inside a lightcone in a classically chaotic system.

In the current system, the OTOCs are influenced by the previously-mentioned odd-even effects. We can once again look only at even sites for sufficiently large L to calculate $\lambda(v)$. Then v_B is the point at which $\lambda(v)$ smoothly goes to 0.

Fig. 5 shows the VDLEs for the right-going and left-going OTOCs. Finite-size effects slightly perturb $\lambda(v)$ around v_B, but we can see that $v_{B,l} \sim 0.7$ and $v_{B,r} \sim 0.85$.

III. CIRCUIT MODELS

I'm going to introduce the $\Gamma(s)$ formalism first and then staircase circuits, but I don't know if I should do it the other way around.

Before discussing asymmetric circuits we will explain how v_B can be extracted from the growth of entanglement. We will show that this method is particularly tractable in the large-q limit before applying this method to staircase circuits. We will see that the butterfly velocities can be made arbitrarily asymmetric by considering long staircases.

Consider a spin chain of N sites, each with dimension q. Sites are labeled by $i = 1, \ldots, N$, while the bonds between sites are labeled by $x = 1, \ldots, N1$. Define the entropy function $S(x)$ as the bipartite entanglement entropy across bond x.

After course-graining, the entanglement becomes a continuous function $S(x, t)$ with maximal slope 1. Given a circuit architecture, the entanglement growth rate is to first order only a function of the slope, so we can write [**?**]

$$\frac{\partial S}{\partial t} = \Gamma\left(\frac{\partial S}{\partial x}\right). \tag{7}$$

It is useful to define the entropy density $s = \partial S/\partial x$, which is so-called because the equilibrium entropy is $S(x,t) = s_{\text{eq}} \min\{x, L - x\}$. In our models $s_{\text{eq}} = 1$.

This function encodes the butterfly velocity as the derivative $\Gamma'(\partial S/\partial x)|_{s_{\text{ext}}}$, where s_{ext} is one of the extremal entropy densities, 1 or -1 in this case. A brief explanation of why this is the case is given in the appendix, while a stronger argument can be found in Ref. [**?**] It follows that any $\Gamma(s)$ with asymmetry at the endpoints will have asymmetric butterfly velocities.

A. Staircase circuits

Subadditivity tells us $|S(x+1) - S(x)| \leq S_1$, where S_1 is the entropy at a single site. If we take our logarithms with base q, then $S_1 \leq 1$.

If a gate acts on bond x, it can increase the bipartite entanglement entropy $S(x)$, up to the constraint $|S(x+1) - S(x)| \leq 1$. In the large-q limit, a Haar-randomly chosen gate will, with probability 1, maximally increase the entanglement across the bond it acts on [70]. Given the previous constraint, this means that if a gate acts at bond x at time t, then $S(x, t+1) = \min\{S(x-1,t)+1, S(x+1,t)+1\}$. Should we explain why? It suffices to consider integer-valued $S(x)$ with $|S(x) - S(x-1)| = 1$ for all x.

Staircase circuits of length n are defined by always having strings of n gates act on sites x through $x+n-1$ in succession. For $n = 1$ this is just a random architecture, but large n results in more asymmetric circuits. Would a figure of the staircase circuit, as in Fig. 38 or 39 in my thesis?

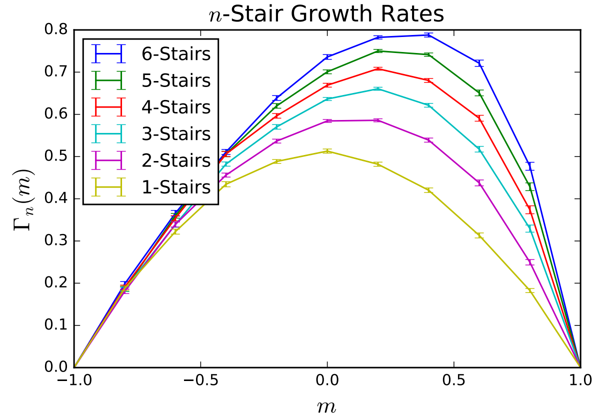

FIG. 6. Empirical growth rate as a function of slope for n-stair circuits. The right/forward and left/backward butterfly velocities are the slopes of these curves at their endpoint, indicating that as the left v_B stays constant, the right v_B increases. The appendix includes an argument that the right v_B is unbounded in the large-n limit.

B. Asymmetric v_B

For small n, we can simulate the circuit directly. For the growth rate curves of n-stair circuits for $n \leq 6$ see Fig. 6. It is possible to approximate these growth rates by assuming the up and down steps are uncorrelated. Then the probability that a randomly placed gate will result in growth is $(1 - s^2)/2$. Any asymmetry comes from the fact that for longer staircases, a gate acting on site x is more likely to have been preceded by a gate on site $x - 1$ so the step from $x - 1$ to x is more likely to be a down step.

Under these assumptions the growth rate is

$$\Gamma_n(s) = \frac{\gamma}{n}\frac{1+s}{1-s}\Bigg((1+s)\left[\left(\frac{1+s}{2}^2\right)^n - 1\right] \\ + n(1-s)\Bigg). \tag{8}$$

This produces successively more asymmetric growth rates as n increases. However, the correlation in the true steady state, and therefore the error of this approximation, also increases. It is possible to correct for the correlation term-by-term in correlation length, but this quickly becomes tedious. For 2-stairs, including the nearest-neighbor correlation removes most of the error in $\Gamma(s)$.

Luckily, as n becomes very large or approaches the size of the system, the correlations again become unimportant. To see this we can consider the growth rate at $s = -1, 0,$ and 1.

The growth rate approaches $\Gamma_\infty = \gamma(s + 1)$, so that for spreading to the left $v_B = 1$ and for spreading to the right $v_B = \infty$. This is of course maximally asymmetric.

IV. CONCLUSION

Advantages of this model: Time-independent Hamiltonian. Only ingredients are chains of two-level systems.

Further work: How do the velocities depend on h? What happens at the phase transition? Maximally asymmetric three-site Hamiltonians? 2-D systems?

ACKNOWLEDGEMENTS

We thank many people.

Note somewhere about arXiv:1809.02614v1

Appendix A: Butterfly velocity from $\Gamma(s)$

To see why $\Gamma'(s_{\text{ext}})$ gives v_B, consider a region in which the entropy profile is piecewise linear, with $S'(x < x^*) = s_1$ and $S'(x > x^*) = s_2$. Also note $\Gamma(s)$ is always convex. This is certainly true for the functions considered above, and is also true in general. Then if $s_1 < 0 < s_2$, the transition between the region stays sharp. If it did not, a curve would form with intermediate slopes $s_1 < S'(x) < s_2$. But from convexity all of this region would have a faster entanglement growth than $\min\{s_1, s_2\}$ and the peak would reform. Furthermore, this peak location x^* travels at velocity $\dot{x}* = -\frac{\Gamma(s_2)-\Gamma(s_1)}{s_2-s_1}$, the slope of the chord connecting $\Gamma(s_2)$ and $\Gamma(s_1)$.

If instead, $s_2 < 0 < s_1$, the kink does not remain sharp. The sharp point x^* becomes a smooth curve, running tangent to the two linear sections at x^*_L and x^*_R. By a similar argument to the above, these features travel at $-\Gamma'(s_{1,2})$. Then the convexity shows that the fastest velocities in the system are $-\Gamma'(s_{\text{ext}})$. It remains to be shown that v_B cannot be slower than this, but this is just an appendix.

[1] J. M. Deutsch, "Quantum statistical mechanics in a closed system," Phys. Rev. A **43**, 2046–2049 (1991).

[2] Mark Srednicki, "Chaos and quantum thermalization," Phys. Rev. E **50**, 888–901 (1994).

[3] Marcos Rigol, Vanja Dunjko, and Maxim Olshanii, "Thermalization and its mechanism for generic isolated quantum systems," Nature **452**, 854–858 (2008).

[4] Immanuel Bloch, Jean Dalibard, and Wilhelm Zwerger, "Many-body physics with ultracold gases," Rev. Mod. Phys. **80**, 885–964 (2008).

[5] Jae-yoon Choi, Sebastian Hild, Johannes Zeiher, Peter Schauß, Antonio Rubio-Abadal, Tarik Yefsah, Vedika Khemani, David A. Huse, Immanuel Bloch, and Christian Gross, "Exploring the many-body localization transition in two dimensions," Science **352**, 1547–1552 (2016).

[6] J. Smith, A. Lee, P. Richerme, B. Neyenhuis, P. W. Hess, P. Hauke, M. Heyl, D. A. Huse, and C. Monroe, "Many-body localization in a quantum simulator with programmable random disorder," ArXiv e-prints (2015), arXiv:1508.07026 [quant-ph].

[7] A. M. Kaufman, M. E. Tai, A. Lukin, M. Rispoli, R. Schittko, P. M. Preiss, and M. Greiner, "Quantum thermalization through entanglement in an isolated many-body system," Science **353**, 794–800 (2016), arXiv:1603.04409 [quant-ph].

[8] P. W. Anderson, "Absence of diffusion in certain random lattices," Phys. Rev. **109**, 1492–1505 (1958).

[9] D. M. Basko, I. L. Aleiner, and B. L. Altshuler, "Metal-insulator transition in a weakly interacting many-electron system with localized single-particle states," Annals of Physics **321**, 1126–1205 (2006).

[10] Arijeet Pal and David A. Huse, "Many-body localization phase transition," Phys. Rev. B **82**, 174411 (2010).

[11] Vadim Oganesyan and David A. Huse, "Localization of interacting fermions at high temperature," Phys. Rev. B **75**, 155111 (2007).

[12] M. Žnidarič, T. Prosen, and P. Prelovšek, "Many-body localization in the Heisenberg XXZ magnet in a random field," Phys. Rev. B **77**, 064426 (2008), arXiv:0706.2539 [quant-ph].

[13] John Z. Imbrie, "On many-body localization for quantum spin chains," Journal of Statistical Physics **163**, 998–1048 (2016).

[14] J. Maldacena, "The Large-N Limit of Superconformal Field Theories and Supergravity," International Journal of Theoretical Physics **38**, 1113–1133 (1999).

[15] E. Witten, "Anti-de Sitter space and holography," Advances in Theoretical and Mathematical Physics **2**, 253–291 (1998), hep-th/9802150.

[16] P. Hayden and J. Preskill, "Black holes as mirrors: quantum information in random subsystems," Journal of High Energy Physics **9**, 120 (2007), arXiv:0708.4025 [hep-th].

[17] Y. Sekino and L. Susskind, "Fast scramblers," Journal of High Energy Physics **10**, 065 (2008), arXiv:0808.2096 [hep-th].

[18] P. Hosur, X.-L. Qi, D. A. Roberts, and B. Yoshida, "Chaos in quantum channels," Journal of High Energy Physics **2**, 4 (2016), arXiv:1511.04021 [hep-th].

[19] S. H. Shenker and D. Stanford, "Black holes and the butterfly effect," Journal of High Energy Physics **3**, 67 (2014), arXiv:1306.0622 [hep-th].

[20] N. Lashkari, D. Stanford, M. Hastings, T. Osborne, and P. Hayden, "Towards the fast scrambling conjecture," Journal of High Energy Physics **4**, 22 (2013), arXiv:1111.6580 [hep-th].

[21] D. A. Roberts, D. Stanford, and L. Susskind, "Localized shocks," Journal of High Energy Physics **3**, 51 (2015), arXiv:1409.8180 [hep-th].

[22] J. S. Cotler, G. Gur-Ari, M. Hanada, J. Polchinski,

P. Saad, S. H. Shenker, D. Stanford, A. Streicher, and M. Tezuka, "Black holes and random matrices," Journal of High Energy Physics **5**, 118 (2017), arXiv:1611.04650 [hep-th].
[23] Daniel A. Roberts and Douglas Stanford, "Diagnosing chaos using four-point functions in two-dimensional conformal field theory," Phys. Rev. Lett. **115**, 131603 (2015).
[24] A Kitaev, "A simple model of quantum holography," Talks at KITP, April 7, 2015 and May 27, 2015. http://online.kitp.ucsb.edu/online/entangled15/kitaev/,http://online.kitp.ucsb.edu/online/entangled15/kitaev2/.
[25] S. Sachdev and J. Ye, "Gapless spin-fluid ground state in a random quantum Heisenberg magnet," Physical Review Letters **70**, 3339–3342 (1993), cond-mat/9212030.
[26] Elliott H. Lieb and Derek W. Robinson, "The finite group velocity of quantum spin systems," Communications in Mathematical Physics **28**, 251–257.
[27] A. I. Larkin and Y. N. Ovchinnikov, "Quasiclassical Method in the Theory of Superconductivity," Soviet Journal of Experimental and Theoretical Physics **28**, 1200 (1969).
[28] J. Maldacena, S. H. Shenker, and D. Stanford, "A bound on chaos," Journal of High Energy Physics **8**, 106 (2016), arXiv:1503.01409 [hep-th].
[29] Y. Gu, X.-L. Qi, and D. Stanford, "Local criticality, diffusion and chaos in generalized Sachdev-Ye-Kitaev models," Journal of High Energy Physics **5**, 125 (2017), arXiv:1609.07832 [hep-th].
[30] Y. Gu and X.-L. Qi, "Fractional statistics and the butterfly effect," Journal of High Energy Physics **8**, 129 (2016), arXiv:1602.06543 [hep-th].
[31] D. Stanford, "Many-body chaos at weak coupling," Journal of High Energy Physics **10**, 9 (2016), arXiv:1512.07687 [hep-th].
[32] A. A. Patel, D. Chowdhury, S. Sachdev, and B. Swingle, "Quantum Butterfly Effect in Weakly Interacting Diffusive Metals," Physical Review X **7**, 031047 (2017), arXiv:1703.07353 [cond-mat.str-el].
[33] D. Chowdhury and B. Swingle, "Onset of many-body chaos in the O (N) model," Phys. Rev. D **96**, 065005 (2017), arXiv:1703.02545 [cond-mat.str-el].
[34] E. B. Rozenbaum, S. Ganeshan, and V. Galitski, "Lyapunov Exponent and Out-of-Time-Ordered Correlator's Growth Rate in a Chaotic System," Physical Review Letters **118**, 086801 (2017), arXiv:1609.01707 [cond-mat.dis-nn].
[35] B. Dóra and R. Moessner, "Out-of-Time-Ordered Density Correlators in Luttinger Liquids," Physical Review Letters **119**, 026802 (2017), arXiv:1612.00614 [cond-mat.str-el].
[36] D. J. Luitz and Y. Bar Lev, "Information propagation in isolated quantum systems," Phys. Rev. B **96**, 020406 (2017), arXiv:1702.03929 [cond-mat.dis-nn].
[37] I. Kukuljan, S. Grozdanov, and T. Prosen, "Weak quantum chaos," Phys. Rev. B **96**, 060301 (2017), arXiv:1701.09147 [cond-mat.stat-mech].
[38] I. L. Aleiner, L. Faoro, and L. B. Ioffe, "Microscopic model of quantum butterfly effect: Out-of-time-order correlators and traveling combustion waves," Annals of Physics **375**, 378–406 (2016), arXiv:1609.01251 [cond-mat.stat-mech].
[39] C.-J. Lin and O. I. Motrunich, "Out-of-time-ordered correlators in quantum Ising chain," ArXiv e-prints (2018), arXiv:1801.01636 [cond-mat.stat-mech].
[40] X. Chen, T. Zhou, D. A. Huse, and E. Fradkin, "Out-of-time-order correlations in many-body localized and thermal phases," Annalen der Physik **529**, 1600332 (2017).
[41] A. Chan, A. De Luca, and J. T. Chalker, "Solution of a minimal model for many-body quantum chaos," ArXiv e-prints (2017), arXiv:1712.06836 [cond-mat.stat-mech].
[42] W. Brown and O. Fawzi, "Scrambling speed of random quantum circuits," ArXiv e-prints (2012), arXiv:1210.6644 [quant-ph].
[43] A. Nahum, S. Vijay, and J. Haah, "Operator Spreading in Random Unitary Circuits," ArXiv e-prints (2017), arXiv:1705.08975 [cond-mat.str-el].
[44] C.W. von Keyserlingk, T. Rakovszky, F. Pollmann, and S. Sondhi, "Operator hydrodynamics, OTOCs, and entanglement growth in systems without conservation laws," ArXiv e-prints (2017), arXiv:1705.08910 [cond-mat.str-el].
[45] T. Rakovszky, F. Pollmann, and C. W. von Keyserlingk, "Diffusive hydrodynamics of out-of-time-ordered correlators with charge conservation," ArXiv e-prints (2017), arXiv:1710.09827 [cond-mat.stat-mech].
[46] V. Khemani, A. Vishwanath, and D. A. Huse, "Operator spreading and the emergence of dissipation in unitary dynamics with conservation laws," ArXiv e-prints (2017), arXiv:1710.09835 [cond-mat.stat-mech].
[47] Jens H. Bardarson, Frank Pollmann, and Joel E. Moore, "Unbounded growth of entanglement in models of many-body localization," Phys. Rev. Lett. **109**, 017202 (2012).
[48] Andrew C. Potter, Romain Vasseur, and S. A. Parameswaran, "Universal properties of many-body delocalization transitions," Phys. Rev. X **5**, 031033 (2015).
[49] Ronen Vosk, David A. Huse, and Ehud Altman, "Theory of the many-body localization transition in one-dimensional systems," Phys. Rev. X **5**, 031032 (2015).
[50] A. Nahum, J. Ruhman, and D. A. Huse, "Dynamics of entanglement and transport in 1D systems with quenched randomness," ArXiv e-prints (2017), arXiv:1705.10364 [cond-mat.dis-nn].
[51] We note that the usual definition of the classical Lyapunov exponent involves averaging the logarithm of the factor by which perturbations grow over initial states and perturbations. This is subtly different from the classical analog of the quantum OTOC where the commutator/Poisson bracket is averaged before taking the logarithm. It is worth exploring in future studies whether or not this difference in definitions has any qualitative consequences[34].
[52] Robert J. Deissler, "One-dimensional strings, random fluctuations, and complex chaotic structures," Physics Letters A **100**, 451 – 454 (1984).
[53] Kunihiko Kaneko, "Lyapunov analysis and information flow in coupled map lattices," Physica D: Nonlinear Phenomena **23**, 436 – 447 (1986).
[54] Robert J. Deissler and Kunihiko Kaneko, "Velocity-dependent lyapunov exponents as a measure of chaos for open-flow systems," Physics Letters A **119**, 397 – 402 (1987).
[55] P. Calabrese and J. Cardy, "Entanglement entropy and conformal field theory," Journal of Physics A Mathematical General **42**, 504005 (2009), arXiv:0905.4013 [cond-mat.stat-mech].
[56] Tomaž Prosen and Iztok Pižorn, "Operator space entanglement entropy in a transverse ising chain," Physical Review A **76**, 032316 (2007).

[57] Iztok Pizorn and Tomaz Prosen, "Operator space entanglement entropy in xy spin chains," arXiv preprint arXiv:0903.2432 (2009).

[58] J Dubail, "Entanglement scaling of operators: a conformal field theory approach, with a glimpse of simulability of long-time dynamics in 1+ 1d," Journal of Physics A: Mathematical and Theoretical **50**, 234001 (2017).

[59] C. Jonay, D.A. Huse, and A. Nahum, Coarse-grained dynamics of operator and state entanglement 1803.00089.

[60] B. Nachtergaele, Y. Ogata, and R. Sims, "Propagation of Correlations in Quantum Lattice Systems," Journal of Statistical Physics **124**, 1–13 (2006), math-ph/0603064.

[61] B. Nachtergaele and R. Sims, "Lieb-Robinson Bounds and the Exponential Clustering Theorem," Communications in Mathematical Physics **265**, 119–130 (2006), math-ph/0506030.

[62] M. B. Hastings and T. Koma, "Spectral Gap and Exponential Decay of Correlations," Communications in Mathematical Physics **265**, 781–804 (2006), math-ph/0507008.

[63] Daniel A. Roberts and Brian Swingle, "Lieb-robinson bound and the butterfly effect in quantum field theories," Phys. Rev. Lett. **117**, 091602 (2016).

[64] Here $\tilde{v}_B(\hat{\mathbf{n}})$, with a tilde, denotes the normal propagation speed of a straight front whose normal is parallel to $\hat{\mathbf{n}}$. In Ref. [43] this was denoted $v_B(\hat{\mathbf{n}})$, but here we use $v_B(\hat{\mathbf{n}})$ to denote the speed at which an initially local operator spreads away from the origin in the direction $\hat{\mathbf{n}}$. These differ because in the absence of rotational symmetry the operator's front is not in general perpendicular to the radial vector, but they are related by a geometrical construction known from classical droplet growth [43, 83, 84].

[65] A. Das, S. Chakrabarty, A. Dhar, A. Kundu, R. Moessner, S. Sankar Ray, and S. Bhattacharjee, "Light-cone spreading of perturbations and the butterfly effect in a classical spin chain," ArXiv e-prints (2017), arXiv:1711.07505 [cond-mat.stat-mech].

[66] R Livi, A Politi, and S Ruffo, "Scaling-law for the maximal lyapunov exponent," Journal of Physics A: Mathematical and General **25**, 4813 (1992).

[67] Kunihiko Kaneko, "Propagation of disturbance, comoving lyapunov exponent and path summation," Physics Letters A **170**, 210–216 (1992).

[68] Arkady S Pikovsky and Jürgen Kurths, "Roughening interfaces in the dynamics of perturbations of spatiotemporal chaos," Physical Review E **49**, 898 (1994).

[69] The expression on the left-hand side of (**??**) becomes a "partition function" for two paths. The local weights $\partial u(\mathbf{y}_{i+1}, i+1)/\partial u(\mathbf{y}_i, i)$ depend not only on $\mathbf{y}_{i+1}$ and $\mathbf{y}_i$ but also on the configuration $u(\mathbf{y_i}, i)$. The chaotic time-dependence of $u(\mathbf{y}_i, i)$ means that the configurational average has a similar effect to averaging over weakly correlated randomness in the weights. Since we are averaging the "partition function", rather than its logarithm, this is an annealed average, and $-\lambda(\mathbf{v})t$ is an annealed "free energy" for the pair of paths. The quenched free energy, in which we take the logarithm before averaging, would give the more conventional definition of the Lyapunov exponent [66–68].

[70] Adam Nahum, Jonathan Ruhman, Sagar Vijay, and Jeongwan Haah, "Quantum entanglement growth under random unitary dynamics," Physical Review X **7**, 031016 (2017).

[71] Inside the light cone there is a large deviation form governing convergence to the saturation value: $C_{1d}^{\mathrm{rc}}(x,t) \sim 1 - \exp\left(-\frac{(v-v_B)^2}{2D}t\right)$. The exponent here is the continuation of $\lambda(v)$ outside the front. However, in the higher dimensional examples, the large deviation form inside the front scales with a distinct power of t, t^d in d spatial dimensions [74]. In the presence of additional conserved densities (like energy or charge), the late time saturation of the OTOC is a power-law in time instead of exponential [45, 46].

[72] In random circuits related random walk pictures underlie the calculation of both the OTOC and the second Renyi entropy [43, 44]. In these random systems this yields a relation between $\lambda(v)$ and the "entanglement line tension" defined in [59], specifically the line tension $\mathcal{E}_2(v)$ for the second Renyi entropy. This motivates the conjecture, for non-random systems, that $\lambda(v)|_{\mathrm{cont}} = -s_{\mathrm{eq}}(\mathcal{E}_2(v) - v)$, where s_{eq} is the thermal entropy density. The left hand side denotes the analytic continuation of $\lambda(v)$ from $v > v_B$ to values $v < v_B$. In random circuits we must distinguish different kinds of averages. The line tension extracted from a calculation of $\overline{e^{-S_2}}$ determines $\lambda(v)$ for the average OTOC $\overline{C(x,t)}$ by the above formula. It is natural to expect that the line tension determined by the more natural direct average $\overline{S_2}$ determines $\lambda(v)$ for the typical value of the OTOC, $\exp \overline{\ln C(x,t)}$. The average and typical values of the OTOC are parametrically close in the region close to the front, but they may differ significantly in the far-front regime where both are exponentially small.

[73] In some circuit models in $d > 1$ (which do not have continuous spatial rotation symmetry) some sections of the operator's front can be "glued" to the strict lightcone defined by the discrete time circuit [43]. This is a peculiar case where $v_B(\hat{\mathbf{n}}) = v_{\mathrm{LC}}(\hat{\mathbf{n}})$ for some directions $\hat{\mathbf{n}}$ in space, so that no nontrivial $\lambda(\mathbf{v})$ can be defined for these directions of $\mathbf{v}$.

[74] P. Le Doussal, S. N. Majumdar, and G. Schehr, "Large deviations for the height in 1D Kardar-Parisi-Zhang growth at late times," EPL (Europhysics Letters) **113**, 60004 (2016), arXiv:1601.05957 [cond-mat.stat-mech].

[75] C. Monthus and T. Garel, "Probing the tails of the ground-state energy distribution for the directed polymer in a random medium of dimension d=1,2,3 via a Monte Carlo procedure in the disorder," Phys. Rev. E **74**, 051109 (2006), cond-mat/0607411.

[76] I. V. Kolokolov and S. E. Korshunov, "Universal and nonuniversal tails of distribution functions in the directed polymer and Kardar-Parisi-Zhang problems," Phys. Rev. B **78**, 024206 (2008), arXiv:0805.0402 [cond-mat.dis-nn].

[77] Andrea Pagnani and Giorgio Parisi, "Numerical estimate of the kardar-parisi-zhang universality class in (2+1) dimensions," Phys. Rev. E **92**, 010101 (2015).

[78] T. Halpin-Healy and K. A. Takeuchi, "A KPZ Cocktail-Shaken, not Stirred..." Journal of Statistical Physics **160**, 794–814 (2015), arXiv:1505.01910 [cond-mat.stat-mech].

[79] Cheng-Ju Lin, Olexei Motrunich, private communication.

[80] Abhishek Dhar, unpublished.

[81] S. Xu and B. Swingle, "Accessing scrambling using matrix product operators," ArXiv e-prints (2018), arXiv:1802.00801 [quant-ph].

[82] Let the probability distribution for weak-link "waiting times" be $P(\tau) \sim \tau^{-a-2}$. At weak disorder $(1 <$

a) the broadening of the operator's front [50] is diffusive, as in the clean system. At intermediate disorder ($0 < a < 1$) the front broadens more strongly, giving $\lambda(v) \sim -(v - v_B)^{(a+1)/a}$. For strong disorder ($-1 < a < 0$) the butterfly speed vanishes: in this regime $\lambda(v) \sim -|v|^{1-|a|}$. In the disordered system the definition of $\lambda(v)$ depends on whether we consider e.g. the mean or the typical value of the OTOC, but this should not change these exponents.

[83] D E Wolf, "Wulff construction and anisotropic surface properties of two-dimensional eden clusters," Journal of Physics A: Mathematical and General **20**, 1251 (1987).

[84] J Krug, H Spohn, and C Godrèche, "in 'solids far from equilibrium'," Solids far from equilibrium (1991).

Should something go here?